PROCEEDINGS OF SCIENCE

PoS(CPOD07)022

Event-by-event transverse momentum fluctuations in nuclear collisions at CERN SPS.

Katarzyna Grebieszkow* **for the NA49 Collaboration**

Warsaw University of Technology
E-mail: kperl@if.pw.edu.pl

The NA49 Collaboration:
C. Alt[9], *T. Anticic*[23], *B. Baatar*[8],*D. Barna*[4], *J. Bartke*[6], *L. Betev*[10], *H. Białkowska*[20], *C. Blume*[9], *B. Boimska*[20], *M. Botje*[1], *J. Bracinik*[3], *R. Bramm*[9], *P. Buncic*[10], *V. Cerny*[3], *P. Christakoglou*[2], *P. Chung*[19], *O. Chvala*[14], *J.G. Cramer*[16], *P. Csató*[4], *P. Dinkelaker*[9], *V. Eckardt*[13], *D. Flierl*[9], *Z. Fodor*[4], *P. Foka*[7], *V. Friese*[7], *J. Gál*[4], *M. Gaździcki*[9,11], *V. Genchev*[18], *G. Georgopoulos*[2], *E. Gładysz*[6], *K. Grebieszkow*[22], *S. Hegyi*[4], *C. Höhne*[7], *K. Kadija*[23], *A. Karev*[13], *D. Kikola*[22], *M. Kliemant*[9], *S. Kniege*[9], *V.I. Kolesnikov*[8], *E. Kornas*[6], *R. Korus*[11], *M. Kowalski*[6], *I. Kraus*[7], *M. Kreps*[3], *A. Laszlo*[4], *R. Lacey*[19], *M. van Leeuwen*[1], *P. Lévai*[4], *L. Litov*[17], *B. Lungwitz*[9], *M. Makariev*[17], *A.I. Malakhov*[8], *M. Mateev*[17], *G.L. Melkumov*[8], *A. Mischke*[1], *M. Mitrovski*[9], *J. Molnár*[4], *St. Mrówczyński*[11], *V. Nicolic*[23], *G. Pálla*[4], *A.D. Panagiotou*[2], *D. Panayotov*[17], *A. Petridis*[2,†], *W. Peryt*[22], *M. Pikna*[3], *J. Pluta*[22], *D. Prindle*[16], *F. Pühlhofer*[12], *R. Renfordt*[9], *C. Roland*[5], *G. Roland*[5], *M. Rybczyński*[11], *A. Rybicki*[6], *A. Sandoval*[7], *N. Schmitz*[13], *T. Schuster*[9], *P. Seyboth*[13], *F. Siklér*[4], *B. Sitar*[3], *E. Skrzypczak*[21], *M. Slodkowski*[22], *G. Stefanek*[11], *R. Stock*[9], *C. Strabel*[9], *H. Ströbele*[9], *T. Susa*[23], *I. Szentpétery*[4], *J. Sziklai*[4], *M. Szuba*[22], *P. Szymanski*[10,20], *V. Trubnikov*[20], *D. Varga*[4,10], *M. Vassiliou*[2], *G.I. Veres*[4,5], *G. Vesztergombi*[4], *D. Vranić*[7], *A. Wetzler*[9], *Z. Włodarczyk*[11], *A. Wojtaszek*[11], *I.K. Yoo*[15], *J. Zimányi*[4,†]

PROCEEDINGS OF SCIENCE

[1]*NIKHEF, Amsterdam, Netherlands.*
[2]*Department of Physics, University of Athens, Athens, Greece.*
[3]*Comenius University, Bratislava, Slovakia.*
[4]*KFKI Research Institute for Particle and Nuclear Physics, Budapest, Hungary.*
[5]*MIT, Cambridge, USA.*
[6]*Henryk Niewodniczanski Institute of Nuclear Physics, Polish Academy of Sciences, Cracow, Poland.*
[7]*Gesellschaft für Schwerionenforschung (GSI), Darmstadt, Germany.*
[8]*Joint Institute for Nuclear Research, Dubna, Russia.*
[9]*Fachbereich Physik der Universität, Frankfurt, Germany.*
[10]*CERN, Geneva, Switzerland.*
[11]*Institute of Physics Świętokrzyska Academy, Kielce, Poland.*
[12]*Fachbereich Physik der Universität, Marburg, Germany.*
[13]*Max-Planck-Institut für Physik, Munich, Germany.*
[14]*Charles University, Faculty of Mathematics and Physics, Institute of Particle and Nuclear Physics, Prague, Czech Republic.*
[15]*Department of Physics, Pusan National University, Pusan, Republic of Korea.*
[16]*Nuclear Physics Laboratory, University of Washington, Seattle, WA, USA.*
[17]*Atomic Physics Department, Sofia University St. Kliment Ohridski, Sofia, Bulgaria.*
[18]*Institute for Nuclear Research and Nuclear Energy, Sofia, Bulgaria.*
[19]*Department of Chemistry, Stony Brook Univ. (SUNYSB), Stony Brook, USA.*
[20]*Institute for Nuclear Studies, Warsaw, Poland.*
[21]*Institute for Experimental Physics, University of Warsaw, Warsaw, Poland.*
[22]*Faculty of Physics, Warsaw University of Technology, Warsaw, Poland.*
[23]*Rudjer Boskovic Institute, Zagreb, Croatia.*
[†]*deceased*

The latest NA49 results on event-by-event transverse momentum fluctuations are presented for central Pb+Pb interactions over the whole SPS energy range (20*A* - 158*A* GeV). Two different methods are applied: evaluating the Φ_{p_T} fluctuation measure and studying two-particle transverse momentum correlations. The obtained results are compared to predictions of the UrQMD model. The results on the energy dependence are compared to the NA49 data on the system size dependence. The NA61 (SHINE, NA49-future) strategy of searching of the QCD critical end-point is also discussed.

Critical Point and Onset of Deconfinement 4th International Workshop
July 9-13 2007
GSI Darmstadt,Germany

[*]Speaker.

PoS(CPOD07)022

1. Motivation

One of the most important reasons to investigate ultra-relativistic heavy ion collisions is to produce and understand the properties of quark-gluon plasma (QGP) - a state of matter, with sub-hadronic degrees of freedom, that is expected to appear when the system is sufficiently hot and dense. The theoretical predictions within the Statistical Model of the Early Stage suggested that the energy threshold for deconfinement is localized between AGS and top SPS energies [1]. Indeed, the latest NA49 results [2] on dependencies of various quantities on the collision energy seem to confirm that the onset of deconfinement sets in at lower SPS energies.

The phase diagram of strongly interacting matter is commonly presented as a (T, μ_B) plot, where T is the temperature and μ_B is a baryochemical potential. For large values of μ_B one expects a first order phase transition between hadron gas and QGP, which terminates in a critical point, and for smaller values of μ_B turns into a so-called crossover. According to the recent lattice QCD calculations, the end-point of the first-order phase transition is a critical point of the second-order and should be located at a baryochemical potential characteristic of the CERN SPS energy range [3].

Dynamical (non-statistical) fluctuations are very important observables in the study of the phase diagram. In this proceedings article, transverse momentum dynamical fluctuations obtained on the basis of event-by-event methods will be presented. **A focus will be put on the energy dependence of p_T fluctuations over the whole SPS energy range**. The two most important reasons of studying the energy dependence of event-by-event p_T fluctuations are:

1. When the studied data sample consists of dynamically very similar events, event-by-event fluctuations are expected to be small. In contrast, when different classes of events are present, the fluctuations from one event to another are obviously much higher (various classes of events may exhibit different global characteristics). The latter situation is more probable for energies close to the phase transition region because QGP may be created only in a fraction of the volume of strongly interacting matter and this fraction can vary from event to event. Therefore, the energy dependence of event-by-event p_T fluctuations might exhibit enlarged fluctuations at lower SPS energies, where the onset of deconfinement probably occurs [1, 2].

2. Significant transverse momentum and multiplicity fluctuations were predicted to appear for systems that hadronize and freeze-out near the second-order critical QCD end-point [4]. The phase diagram can be scanned by varying both the energy and the system size and therefore a non-monotonic dependence of p_T and N fluctuations on control parameters such as energy or centrality (ion size) may provide evidence for the QCD critical point.

2. Measures of transverse momentum fluctuations

There are several methods that can be used to determine p_T fluctuations on event-by-event basis. In the NA49 experiment the Φ_{p_T} fluctuation/correlation [1] measure, proposed in [5], is studied

[1] Several effects may lead to non-zero value of Φ_{p_T}. Among them are those which occur on an event-by-event basis (event-by-event fluctuations of the inverse slope parameter, existence of different event classes i.e. 'plasma' and 'normal' events), but also inter-particle correlations due to Bose-Einstein statistics, Coulomb effects, resonance decays, flow, jet production etc.

(for a complete definition of Φ_{p_T} see [5] and the publication of NA49 [6]). Φ_{p_T} quantifies a difference between event-by-event fluctuations of transverse momentum in data and the corresponding fluctuations in 'mixed' events. There are two important properties of the Φ_{p_T} measure. When the system consists of independently emitted particles (no inter-particle correlations) Φ_{p_T} assumes a value of zero. On the other hand, if A+A collisions can be treated as an incoherent superposition of independent N+N interactions (superposition model), then Φ_{p_T} has a constant value, the same for A+A and N+N interactions.

Although Φ_{p_T} measures the magnitude of fluctuations it does not provide information on the source of underlying correlations. Therefore a more differential method (suggested in [7]) is also applied and two-particle correlation plots (x_1, x_2), using the cumulant p_T variable x, are prepared (technical details can be found in [6]). Those two-dimensional plots are *uniformly* populated when no inter-particle correlations are present in the system and a possible non-uniform structure signals the presence of dynamical fluctuations (for example, Bose-Einstein correlations lead to a ridge along the diagonal of the (x_1, x_2) plot, which starts at $(0,0)$ and ends at $(1,1)$, whereas event-by-event temperature fluctuations produce a saddle shaped structure [7, 6]).

3. NA49, data selection and analysis

The NA49 fixed target experiment is a large hadron spectrometer at the CERN SPS. The main devices of the detector are four large volume Time Projection Chambers (TPCs). The Vertex TPCs (VTPC-1 and VTPC-2) are located in the magnetic field of two super-conducting dipole magnets. Two other TPCs (MTPC-L and MTPC-R) are positioned downstream of the magnets symmetrically to the beam line. The NA49 TPCs allow precise measurements of particle momenta p with a resolution of $\sigma(p)/p^2 \cong (0.3-7)\cdot 10^{-4}$ (GeV/c)$^{-1}$. Precise measurement of specific energy loss (dE/dx) in the region of relativistic rise is possible in the TPCs, however, dE/dx information is not used in this analysis. The centrality of the nuclear collisions is selected by use of information from a downstream calorimeter (VCAL), which measures the energy of the projectile spectator nucleons. Details of the NA49 detector set-up and performance of the tracking software are described in [9].

The data used for the analysis consists of samples of Pb+Pb collisions at 20*A*, 30*A*, 40*A*, 80*A* and 158*A* GeV energy ($\sqrt{s_{NN}}$ = 6.27, 7.62, 8.73, 12.3 and 17.3 GeV, respectively). The fraction of the total inelastic cross section of nucleus+nucleus collisions (σ/σ_{tot}) was set to 7.2%. The fluctuation analysis presented in these proceedings is performed by use of all charged particles, registered by the NA49 detector at forward rapidity. Additionally, the results are prepared for negatively and positively charged particles, separately. In the analysis tracks with $0.005 < p_T < 1.5$ GeV/c are used. For all five energies the forward rapidity region is selected as $1.1 < y^*_\pi < 2.6$, where y^*_π is the particle rapidity calculated in the center-of-mass reference system. As the track-by-track identification is not always possible in the experiment, the rapidities are calculated assuming pion mass for all particles.

Fig. 1 presents examples of azimuthal angle versus p_T (ϕ, p_T) acceptance for all charged particles [2] at $2.0 < y^*_\pi < 2.2$. The regions of complete azimuthal acceptance *common* for all energies are denoted by black solid lines and described by an analytical formula: $p_T(\phi) = \frac{A}{\phi^2} - B$, where

[2] In the NA49 detector positively charged particles are concentrated around $\phi = 0^o$, whereas negatively charged ones close to $\phi = \pm 180^o$ (standard configuration of the magnetic field). Therefore in the plot, azimuthal angle of negatively

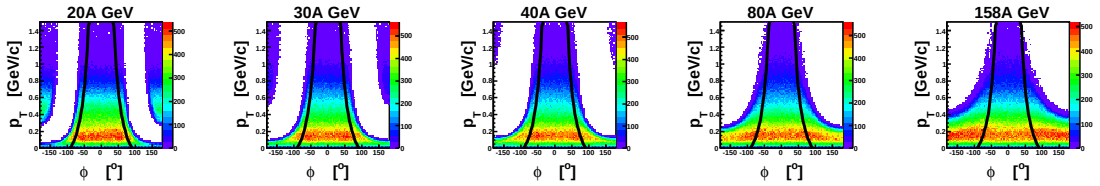

Figure 1: NA49 (ϕ, p_T) acceptance of all charged particles for $2.0 < y^*_\pi < 2.2$. Additional cut on y^*_p (see the text) not included. The solid lines represent the analytical parametrization of the common acceptance.

y^*_π	1.0-1.2	1.2-1.4	1.4-1.6	1.6-1.8	1.8-2.0	2.0-2.2	2.2-2.4	2.4-2.6
$A[\frac{deg.^2 GeV}{c}]$	600	700	1000	2600	3000	2500	1800	1000
$B[\frac{GeV}{c}]$	0.2	0.2	0.2	0.5	0.4	0.3	0.3	0.1

Table 1: The parametrization of the NA49 $\phi - p_T$ acceptance common for all five energies.

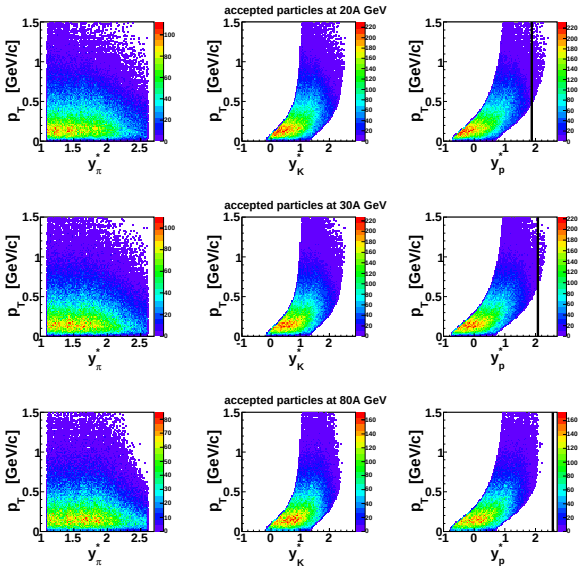

Figure 2: (y^*, p_T) plots of all accepted particles assuming pion (left), kaon (middle) and proton (right) mass. Additional cut on y^*_p (see the text) is not included. Top, middle and bottom panels correspond to 20*A*, 30*A* and 80*A* GeV data, respectively. Black lines represent beam rapidities (y^*_{beam}) in the center-of-mass reference system.

the parameters A and B depend on the rapidity range as given in Table 1. Only particles within the analytical curves are used in the analysis.

Fig. 2 presents (y^*, p_T) plots of all charged particles accepted in the analysis (additional cut on y^*_p - see below - not included in the plots). It can be seen that at lower energies the NA49 TPC acceptance extends to the projectile spectator domain. This domain was excluded by an additional cut $y^*_p < y^*_{beam} - 0.5$ (see below).

The methods of determining statistical and systematic errors can be found in [6]. Systematic errors have been determined from Φ_{p_T} stability for different event and track selection criteria.

charged particles is reflected: namely for particles with $\phi < 0^o$ the azimuthal angle is changed as follows:$\phi = \phi + 360^o$, and finally $\phi = \phi - 180^o$.

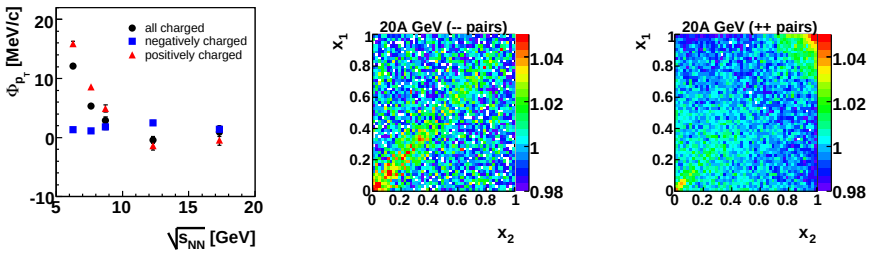

Figure 3: NA49 results without additional cut: $y^*_p < y^*_{beam} - 0.5$. Φ_{p_T} versus energy (left) and two-particle correlation plots (x_1, x_2) using the cumulant p_T variable x for 20A GeV interactions for pairs of negatively charged particles (middle) and positively charged ones (right).

The influence of random losses of particles (reconstruction inefficiency, track cuts) on Φ_{p_T} values has been checked and found to be very small in the studied kinematic region. The influence of the limited two-track resolution (TTR) of the NA49 detector has been determined on the basis of 'mixed' events and Geant simulations (details of the procedure can be found in [6]). In the studied kinematic and acceptance region the values of those corrections are not higher than 4 MeV/c (for top SPS energy) and those additive corrections have been applied to 'raw' Φ_{p_T} values.

The preliminary analysis of the energy dependence of p_T fluctuations showed a strong increase of Φ_{p_T} for *positively charged* particles at lower SPS energies (Fig. 3 (left)). Also two-particle correlation plots for the lowest SPS energy, exhibited an additional source (peak at high x) beyond Bose-Einstein and Coulomb correlations on the diagonal, but for positively charged particles only (Fig. 3 (right)). The UrQMD model qualitatively confirmed the structures observed in Fig. 3 (left). Moreover, both the UrQMD model and the NA49 data (Fig. 4) with dE/dx identification agree that only *protons* are responsible for the observed effect, whereas Φ_{p_T} for newly produced particles such as kaons, pions, anti-protons is consistent with zero. Finally, it was found that this surprising effect can be explained by event-by-event impact parameter fluctuations or more precisely by a correlation between the number of protons in the forward hemisphere and the number of protons in the production region. One can eliminate this trivial source of correlations either by centrality restriction (Fig. 5) or by rejection of the beam spectator region (Fig. 6). In the analysis of the NA49 data the rejection method is employed by applying a cut on y^*_p at each energy, i.e. the rapidity y^*_p calculated with the proton mass is required to be lower than $y^*_{beam} - 0.5$, where y^*_{beam} is the beam rapidity in the center-of-mass reference system.

4. Results and discussion, comparison to the UrQMD model

The fluctuation measure Φ_{p_T}, as a function of energy, is shown in Fig. 7. Three panels represent all charged, negatively charged and positively charged particles, respectively. Points correspond to data (with statistical and systematic errors) and lines to predictions of the UrQMD model [10, 11] with the same centrality, kinematic and acceptance restrictions as in the data. For all three charge combinations no significant energy dependence of the Φ_{p_T} measure can be observed, both for data and for the UrQMD events. Moreover, Φ_{p_T} values are consistent with the hypothesis of independent particle production (close to zero). The energy dependence of the Φ_{p_T} measure

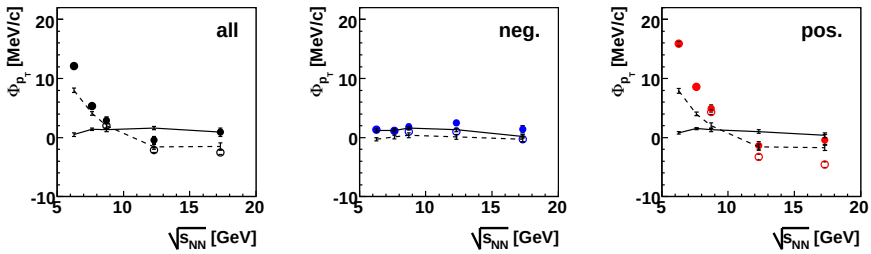

Figure 4: Φ_{p_T} as a function of energy calculated for *not* identified particles without two-track resolution corrections (open points) and with two-track resolution corrections (full points) compared to identified pions (solid curves) and (anti-)protons (dashed curves). Results for identified particles *do not* include two-track resolution corrections. Additional cuts on dE/dx values and the total momentum ($p \geq 3$ GeV/c) were applied for proton and pion identification. The panels represent: all charged, negatively charged, positively charged particles, respectively.

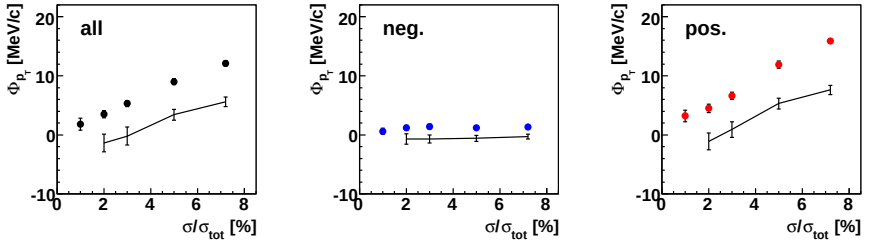

Figure 5: Φ_{p_T} for the most central 20*A* GeV Pb+Pb interactions as a function of the fraction of the total inelastic cross section of nucleus+nucleus collisions (σ/σ_{tot}). Points represent NA49 data with kinematic and acceptance cuts as described above (without y^*_p cut). Black lines correspond to the UrQMD model with the acceptance restrictions the same as for data. Data points are *not* corrected for the limited two-track resolution. The panels represent: all charged, negatively charged, positively charged particles, respectively. Note: the values and their errors are correlated.

does not show any anomalies which might appear when approaching the phase boundary or the critical point.

Two-particle correlation plots (for all charged particles) of the cumulant transverse momentum variable x are presented in Fig. 8 for 20*A*, 30*A*, 40*A*, 80*A* and 158*A* GeV central Pb+Pb collisions. The plots are not uniformly populated but the same structure can be observed for all SPS energies. The enhancement of the point density in the region close to the diagonal is attributed to short range (Bose-Einstein and Coulomb) correlations.

It was suggested in [4] that fluctuations due to the critical QCD point should be dominated by fluctuations of pions with low transverse momenta (approximately below 500 MeV/c). Fig. 9 shows the dependence of Φ_{p_T} on energy for several choices of an upper p_T cut. One can see that no significant energy dependence of the Φ_{p_T} measure can be observed, also when low transverse momenta are selected. There are no anomalies exhibited and the measured Φ_{p_T} values are not significantly increased as it might be expected when the freeze-out takes place in the vicinity of the critical point. It should be pointed out that the predicted fluctuations at the critical point should result in $\Phi_{p_T} \approx 20$ MeV/c, but the effect of limited acceptance of NA49 (forward rapidity) reduces them to $\Phi_{p_T} \approx 10$ MeV/c [4].

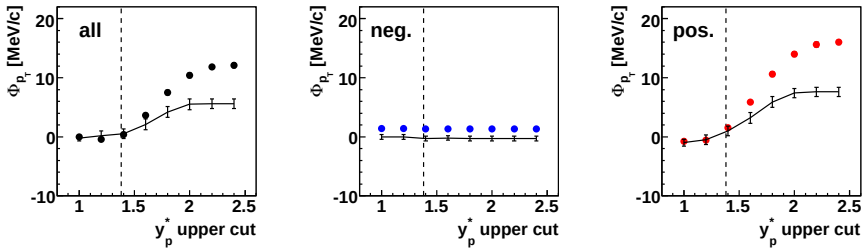

Figure 6: Φ_{p_T} as a function of an upper y_p^* cut, obtained for 20*A* GeV interactions. Points represent NA49 data with kinematic and acceptance cuts as described above (without y_p^* cut). Black lines correspond to the UrQMD model with the acceptance restrictions the same as for data. Data points are *not* corrected for the limited two-track resolution. The panels represent: all charged, negatively charged, positively charged particles, respectively. For 20*A* GeV interactions y^*_{beam}=1.88. Note: the values and their errors are correlated. The dashed lines indicate the y_p^* cuts used in the analysis of 20*A* GeV data.

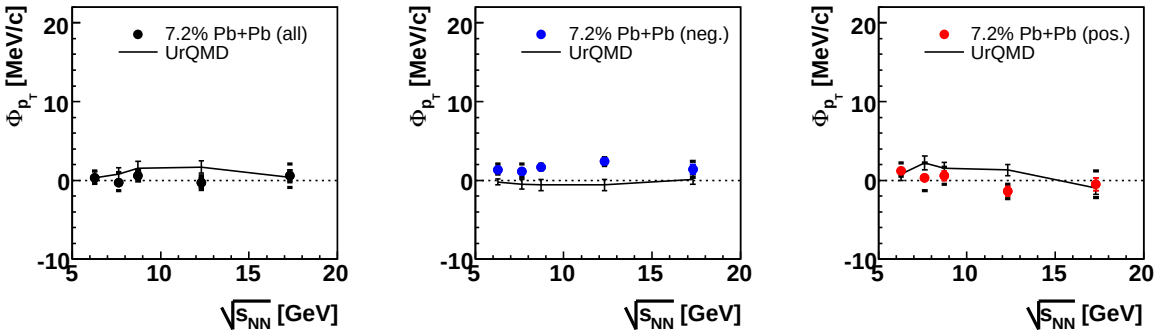

Figure 7: Φ_{p_T} as a function of energy for the 7.2% most central Pb+Pb interactions for all charged particles (left) and for negatively charged (middle) and positively charged ones (right). Data points are corrected for the limited two-track resolution. Points are shown with statistical and systematic errors. NA49 results are compared to the UrQMD predictions (lines) with the acceptance restrictions.

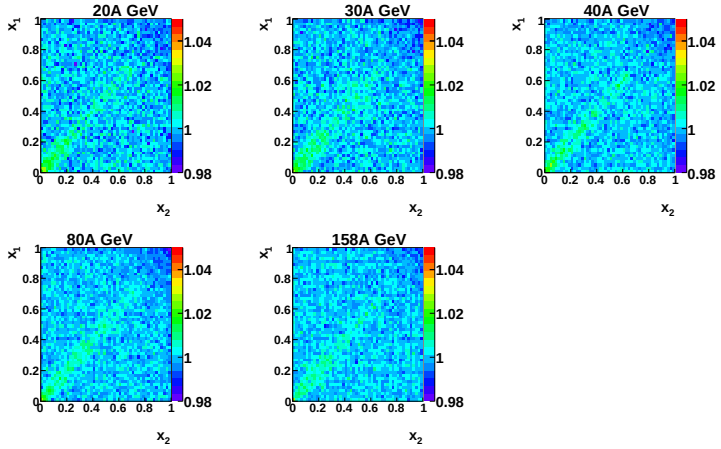

Figure 8: Two-particle correlation plots (x_1, x_2) using the cumulant p_T variable x. The bin contents are normalized by dividing with the average number of entries per bin. Plots are for all charged particles produced in central Pb+Pb collisions at 20*A* - 158*A* GeV.

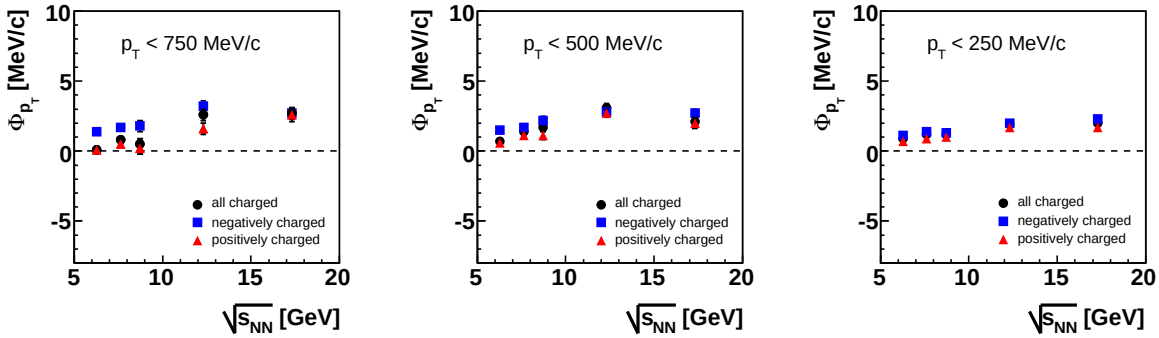

Figure 9: Φ_{p_T} as a function of energy for the 7.2% most central Pb+Pb interactions. Results with additional cuts $p_T < 750$ MeV/c (left), $p_T < 500$ MeV/c (middle) and $p_T < 250$ MeV/c (right). Data points are corrected for the limited two-track resolution. Errors are statistical only.

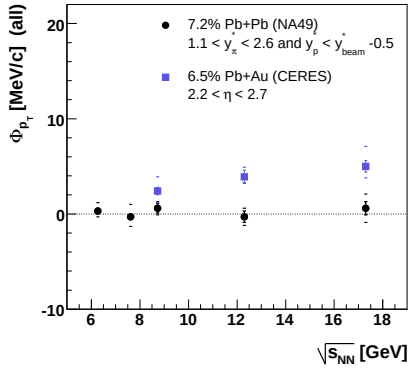

Figure 10: Φ_{p_T} as a function of energy measured for all charged particles by NA49 and CERES experiments. The NA49 points are obtained for the forward rapidity region in a limited azimuthal angle acceptance; the CERES data [12] are calculated for the mid-rapidity region within a complete azimuthal acceptance.

5. Comparison with other experiments

Event-by-event transverse momentum fluctuations have been studied by other experiments both at SPS and at RHIC energies. Fig. 10 shows the comparison of NA49 and CERES [12] results on the energy dependence of the Φ_{p_T} measure. One can observe only very weak (if any) energy dependence of Φ_{p_T} over the whole SPS energy range. It should be however stressed that quantitative comparison of Φ_{p_T} values in NA49 and CERES is obscured by different acceptances of both experiments (NA49 - forward rapidity and limited azimuthal angle, CERES - mid-rapidity and complete azimuthal acceptance).

Although the Φ_{p_T} measure seems to be close to zero at SPS energies, the latest STAR [13] results show strong increase of Φ_{p_T} from top SPS to RHIC energies (up to 50 MeV/c at top RHIC energy). This effect, however, can be related to increased contribution from (mini-)jet production. A non-monotonic behavior of p_T fluctuations with collision energy (the probable effect of approaching the phase boundary or indication of the hadronization near the critical point) have not been observed neither at SPS nor at RHIC energy.

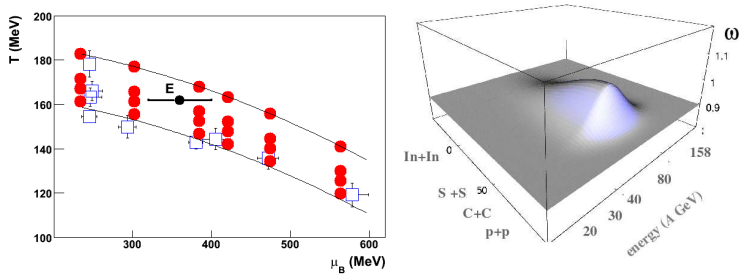

Figure 11: Left: Hypothetical positions of the chemical freeze-out points in the NA61 calculated using parametrization in [18]. Predictions for InIn, SS, CC, pp (from bottom to top) and for 158A, 80A, 40A, 30A, 20A, 10A GeV (from left to right). Open squares correspond to existing NA49 data. Position of the critical point (E) taken from [3]. Right: Outline of the critical point search strategy in NA49 and NA61 experiments. The scaled variance ω [15] represents multiplicity fluctuations.

6. Looking for the critical point in the NA61 experiment

The latest NA49 results on the energy dependence of p_T fluctuations in central Pb+Pb collisions seem to leave no place for anomalies suggestive of an approach to the phase boundary and for effects of the critical point. However, the NA49 experiment measured significant non-monotonic evolution of Φ_{p_T} with the system size at top SPS energy [6]. This tendency was also confirmed by the CERES experiment [14]. Moreover, an increase of multiplicity fluctuations for peripheral Pb+Pb interactions (when compared to p+p and central Pb+Pb collisions) was measured by NA49 [15]. Both observations [3] might be the first indication of the critical point.

The above results provided powerful arguments for a new experiment at CERN SPS - NA61 (SHINE), which is an already approved successor of the NA49 [16, 17]. The NA61 experiment plans to study collisions of light and intermediate mass nuclei in order to cover a broad range of the phase diagram (Fig. 11 (left)). Fig. 11 (right) shows schematically critical point search strategy. Critical point can lead to an increase of N and p_T fluctuations provided the freeze-out takes place in its vicinity ($\Delta T \approx 10$ MeV, $\Delta\mu_B \approx 50$ MeV [19]) and therefore the results from NA49 and NA61 may show a 'hill' of fluctuations over the smoothly varying background.

Fig. 12 presents the current status of the NA49 analysis, where the system size dependence at the top SPS energy is shown, as well as the energy dependence for the most central interactions over the whole SPS energy range. The analysis of the system size dependence at 40A GeV is currently in progress. In Fig. 13 the UrQMD predictions for the NA61 data are shown. The computation has been prepared for negatively charged particles at forward rapidities. The right panel of Fig. 13 demonstrates simplified expectations for the presence of the critical end-point.

The latest promising results from SPS experiments motivated also RHIC to decrease energies down to the values $\sqrt{s_{NN}}$ = 5-15 GeV [20]. Suitably to the RHIC project the JINR and GSI laboratories intend to increase their energies that would allow for a formation of a strongly interacting mixed quark-hadron phase [21, 22]. The full review of heavy-ion facilities, of course, should mention the LHC machine which will provide heavy-ion interactions at nearly baryon-free region i.e. at very low μ_B values. The future results, together with the existing data, would allow to cover a

[3] Simultaneous observation of fluctuations in p_T and multiplicity with a maximum at similar $\langle N_W \rangle$ (mean number of wounded nucleons) as predicted for the critical point.

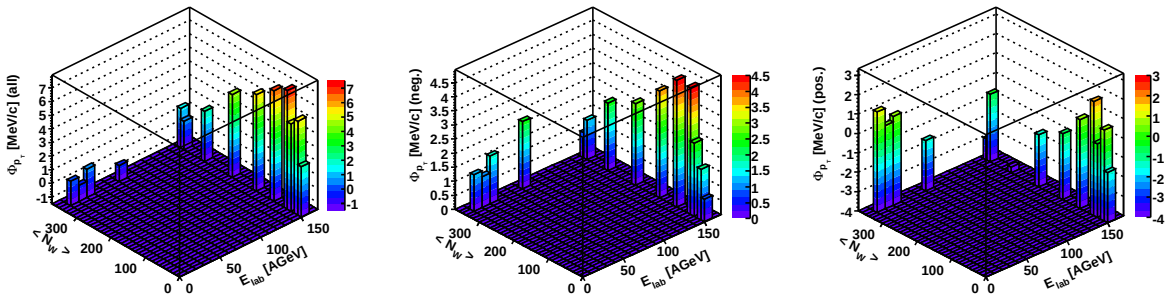

Figure 12: Φ_{p_T} as a function of energy and number of wounded nucleons for all charged (left), negatively charged (middle) and positively charged (right) particles. Errors are not shown. Note: different color scales; different azimuthal angle acceptance for the energy scan and for the system size dependence at 158*A* GeV.

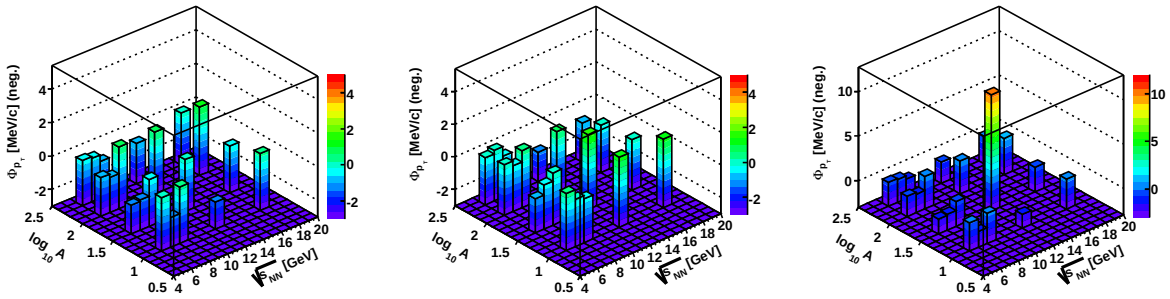

Figure 13: Φ_{p_T} as a function of energy and atomic number (A) for forward rapidity negatively charged particles obtained from the UrQMD model. Statistical errors (not shown) are on the level of 0.5 - 1.0 MeV/c. Left: Calculations for common (for all energies and systems), limited azimuthal angle acceptance (the same as described in this paper). Middle: Calculations with no azimuthal angle restrictions. Right: the same Φ_{p_T} values as in the left panel, but value for 80A GeV S+S interactions is artificially increased by 10 MeV/c - a magnitude predicted by theorists for the NA49 acceptance (forward rapidity) [4].

broad range in the (T, μ_B) plane and may help to confirm, discover or rule out the existence of the critical point in the SPS domain.

Acknowledgments

This work was supported by the US Department of Energy Grant DE-FG03-97ER41020/A000, the Bundesministerium fur Bildung und Forschung, Germany, the Virtual Institute VI-146 of Helmholtz Gemeinschaft, Germany, the Polish State Committee for Scientific Research (1 P03B 006 30, 1 P03B 097 29 , 1 PO3B 121 29, 1 P03B 127 30), the Hungarian Scientific Research Foundation (T032648, T032293, T043514), the Hungarian National Science Foundation, OTKA, (F034707), the Polish-German Foundation, the Korea Science & Engineering Foundation (R01-2 005-000-10334-0), the Bulgarian National Science Fund (Ph-09/05) and the Croatian Ministry of Scie nce, Education and Sport (Project 098-0982887-2878).

References

[1] M. Gazdzicki and M. I. Gorenstein, *On the early stage of nucleus-nucleus collisions*, *Acta Phys. Polon.* **B30**, 2705 [hep-ph/9803462].

[2] C. Alt et al. (NA49 Collab.), *Pion and kaon production in central Pb + Pb collisions at 20-A and 30-A-GeV: Evidence for the onset of deconfinement*, [arXiv:0710.0118[nucl-ex]].
M. Mitrovski et al. (NA49 Collab.), *Strangeness production at SPS energies*, *J. Phys.* **G32**, S43 [nucl-ex/0606004].
S. V. Avanasiev et al. (NA49 Collab.), *Energy dependence of pion and kaon production in central Pb + Pb collisions*, *Phys. Rev.* **C66**, 054902 [nucl-ex/0205002].

[3] Z. Fodor and S. D. Katz, *Critical point of QCD at finite T and μ, lattice results for physical quark masses*, *JHEP* **0404**, 050 [hep-lat/0402006].

[4] M. Stephanov, K. Rajagopal, and E. V. Shuryak, *Event-by-event fluctuations in heavy ion collisions and the QCD critical point*, *Phys. Rev.* **D60**, 114028 [hep-ph/9903292], and private communication.

[5] M. Gazdzicki and St. Mrowczynski, *A method to study 'equilibration' in nucleus-nucleus collisions*, *Z. Phys.* **C54**, 127 (1992).

[6] T. Anticic et al. (NA49 Collab.), *Transverse Momentum Fluctuations in Nuclear Collisions at 158 AGeV*, *Phys. Rev.* **C70**, 034902 [hep-ex/0311009].

[7] T. Trainor, *Event-by-event analysis and the central limit theorem*, hep-ph/0001148.

[8] A. Bialas and M. Gazdzicki, *A new variable to study intermittency*, *Phys. Lett.* **B252**, 483 (1990).

[9] S. Afanasiev et al. (NA49 Collab.), *The NA49 large acceptance hadron detector*, *Nucl. Instrum. Meth.* **A430**, 210 (1999).

[10] S. A. Bass et al., *Microscopic Models for Ultrarelativistic Heavy Ion Collisions*, *Prog. Part. Nucl. Phys.* **41**, 225 [nucl-th/9803035].

[11] M. Bleicher et al., *Relativistic Hadron-Hadron Collisions and the Ultra-Relativistic Quantum Molecular Dynamics Model (UrQMD)*, *J. Phys.* **G25**, 1859 [hep-ph/9909407].

[12] D. Adamova et al. (CERES Collaboration), *Event-by-event fluctuations of the mean transverse momentum in 40, 80, and 158 AGeV/c Pb-Au collisions*, *Nucl. Phys.* **A727**, 97 [nucl-ex/0305002].

[13] J. Adams et al. (STAR Collab.), *The energy dependence of p_t angular correlations inferred from mean-p_t fluctuation scale dependence in heavy ion collisions at the SPS and RHIC*, *J.Phys.* **G33**, 451 [nucl-ex/0605021].

[14] H. Sako and H. Appelshauser (for the CERES Collab.), *Event-by-event Fluctuations at 40, 80 and 158 AGeV/c in Pb+Au Collisions*, *J. Phys.* **G30**, S1371 [nucl-ex/0403037].

[15] C. Alt et al. (NA49 Collab.), *Centrality and system size dependence of multiplicity fluctuations in nuclear collisions at 158A GeV*, *Phys. Rev.* **C75**, 064904 [nucl-ex/0612010].

[16] N. Antoniu et al. (NA49-future Collab.), *Study of Hadron Production in Hadron-Nucleus and Nucleus-Nucleus Collisions at the CERN SPS*, CERN-SPSC-2006-034 and SPSC-P-330 (2006).

[17] M. Gazdzicki (for the NA49-future Collab.), *A new SPS programme*, *PoS*, **CPOD2006**, 016 [nucl-ex/0612007].

[18] F. Becattini, J. Manninen, M. Gazdzicki, *Energy and system size dependence of chemical freeze-out in relativistic nuclear collisions*, *Phys. Rev* **C73**, 044905 [hep-ph/0511092].

[19] Y. Hatta and T. Ikeda, *Universality, the QCD critical/tricritical point and the quark number susceptibility*, *Phys. Rev.* **D67**, 014028 [hep-ph/0210284].

[20] P. Sorensen (for the STAR Collab.), *RHIC Critical Point Search: Assessing STAR's Capabilities*, *PoS*, **CPOD2006**, 019 [nucl-ex/0701028].
J. T. Mitchell (for the PHENIX Collab.), *The PHENIX Potential in the Search for the QCD Critical Point*, nucl-ex/0701079.

[21] A. N. Sissakian, A. S. Sorin, and V. D. Toneev, *QCD Matter: A Search for a Mixed Quark-Hadron Phase*, nucl-th/0608032.

[22] V. Friese, *The CBM experiment at FAIR*, these proceedings.